[5]

Effects of structural relaxation on cationic tracer diffusion in silicate melts

DONALD B. DINGWELL

Bayerisches Geoinstitut, Universität Bayreuth, D-8580 Bayreuth (Federal Republic of Germany)

(Received August 14, 1989; revised and accepted December 29, 1989)

Abstract

Dingwell, D.B., 1990. Effects of structural relaxation on cationic tracer diffusion in silicate melts. Chem. Geol., 82: 209–216.

The glass transition in silicate melts is a curve in time–temperature space marking the transition of the melt structure from an unrelaxed, disequilibrium glass to a relaxed, equilibrium liquid. Tracer diffusivity data obtained in glasses vs. liquids cannot be compared without consideration of the effects of this transition. For tracer diffusivity experiments, two time scales are important, the time duration of the experiment (τ_d) and the inverse of the jump frequency (τ_p) of the tracer.

When the time duration of the experiments reaches the relaxation time-scale ($\tau_d = \tau_s$) of the melt a transition occurs from diffusion in an unrelaxed matrix (undergoing vibrational thermal expansion) to diffusion in a relaxed matrix (undergoing equilibrium, configurational and elastic, thermal expansion). At this transition, an inflection is observed in the temperature dependence of cationic tracer diffusivity. At temperatures below the inflection, the diffusivity is Arrhenian whereas at temperatures above the diffusivity is non-Arrhenian.

At high temperatures the tracer diffusivities of the cations approach the value of diffusivity obtained from the Eyring relation ($\tau_p = \tau_s$). The contrasting, high-temperature, composition dependence of Na and Li vs. Co, Cs, Sr, Ba, Eu, Fe and C diffusivities can be explained in terms of the Eyring (network O and Si) diffusivity influencing the latter group. The contrasting high- vs. low-temperature, composition dependence of Ba and Sr diffusivities can be similarly explained. These latter observations indicate that all cationic diffusivities will be within a $\log_{10}$ unit of the Eyring oxygen diffusivity in melts with viscosities below 10 P.

1. Introduction

Recent ^{29}Si NMR studies on the spin–spin relaxation of Si in silicate melts (Liu et al., 1988; Stebbins, 1988) have demonstrated that the lifetime of a Si–O bond in a silicate liquid corresponds to the macroscopically defined glass transition (i.e. the time-scale of relaxation of the melt structure to changes in density, shear stress, temperature). This time-scale also corresponds to the jump frequency of oxygen diffusion and is related to the onset of unrelaxed, non-Newtonian shear flow in silicate liquids (Li

and Uhlmann, 1970; Simmons et al., 1982; Dingwell and Webb, 1989, 1990; Webb and Dingwell, 1990a, b), supporting the inference that the basic unit of viscous flow and oxygen diffusion in silicate liquids is an oxygen anion. These observations help to explain the success of the Eyring equation,

$$D = kT/\lambda\eta \qquad (1)$$

(where k is Boltzmann's constant, T is temperature, λ is an effective jump distance and η is viscosity; Glasstone et al., 1941) in relating viscosity to O and Si diffusivity in silicate liquids

(e.g., Brebec et al., 1980; Shimizu and Kushiro, 1984).

In this paper, two consequences of structural relaxation on cationic tracer diffusivity are illustrated. The first consequence has been previously recognized in the glass literature (e.g., Haven and Verkerk, 1965). It concerns the dwell time or duration (τ_d) of diffusion experiments with respect to the structural relaxation time-scale and must be distinguished from a second consequence that concerns the relative diffusion time-scales of network O and Si (τ_s) and the cations of interest (τ_p).

The present analysis of the latter provides a simple, dynamic explanation for: (1) the contrasting composition dependence of different tracer cations; (2) the contrasting low- vs. high-temperature composition dependence of diffusivity of some cations; and (3) the similarity in tracer diffusivity of a chemically diverse group of elements, in geologic melts.

2. Structural relaxation

Volume relaxation is the process of equilibration of the density of volume of a matrix to a change in temperature or pressure. Following a change in temperature, the response of the volume of the sample to the new equilibrium value follows a time-dependent path that may be divided into an instantaneous (10^{-13} s, elastic) component and a slower (viscous) component. Microscopically, the elastic response may be viewed as the vibrational component of expansivity and the viscous component as the translational/configurational component. Analogous models can be used for shear relaxation and enthalpy relaxation, and the term "structural relaxation" can be used to describe all three (e.g., Scherer, 1984). The time-scale of volume relaxation decreases with increasing temperature and a volume relaxation curve in temperature–time space can be constructed for each melt composition based on studies of volume relaxation following temperature changes (Ritland, 1954) or pressurization (Höfler and

Seifert, 1984). One point on this curve is the glass transition "temperature", T_g, traditionally measured at a single experimental time-scale using dilatometry (shear or volume relaxation) or calorimetry (enthalpy relaxation). It has been proposed (Dingwell and Webb, 1989) that these relaxation curves may be predicted for silicate melts, within a $\log_{10}$ unit of time, using the mechanical model of a Maxwell element, (i.e. a Hookean spring and a Newtonian dashpot in series). The relaxation time for such a model is simply:

$$\tau = \eta/M \qquad (2)$$

where τ is the relaxation time; η is the viscosity; and M is the elastic modulus. Because the time scale of structural relaxation has been identified with the inverse of the jump frequency of oxygen in Si–O bonds (Liu et al., 1988; Stebbins, 1988). The volume relaxation time-scale, macroscopically derived, can be used to estimate O and Si diffusivity, rate-limited by this mechanism (Dingwell and Webb, 1989).

3. Fast relaxation

The relaxation of certain components of silicate melts can be detached from the time-scale of structural relaxation. Alkali tracer diffusivity data indicate that alkali diffusion can proceed with jump frequencies that are much higher than oxygen jump frequencies (e.g., Johnson et al., 1951). The alkali mobility is said to be "decoupled" (Angell, 1988) from the silicate matrix and the temperature dependence of alkali mobility describes its own curve, separate from the structural relaxation curve. This "fast" relaxation curve corresponds to the time-scale of the alkali diffusive jump and is a relaxation time-scale for electrical conductivity in silicate melts (e.g., Provenzano et al., 1972).

4. Experimental time-scale (τ_d)

Fig. 1 is a summary of experimental data concerning structural and fast relaxation in a $Na_2O-3SiO_2$ melt. The structural relaxation curve is determined by the shear viscosity data
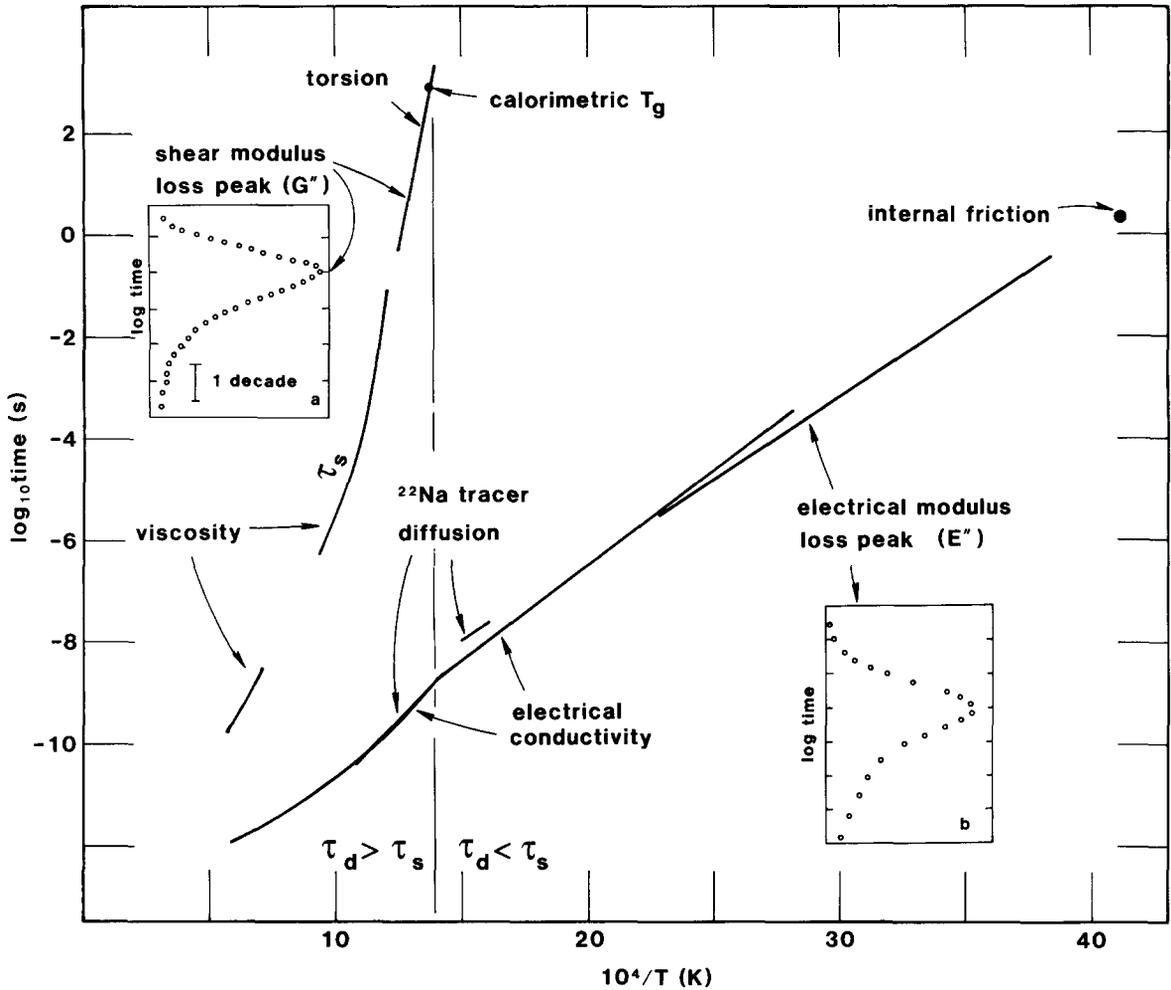
Fig. 1. Relaxation time-scales in $Na_2O-3SiO_2$ melt. The inflection in electrical and diffusion data at T_g result from the experimental duration (τ_d) approaching the structural relaxation time-scale (τ_s). Structural relaxation data from the torsional study of Mills (1974) and the viscosity studies of Poole (1948) and Bockris et al. (1955). Alkali and electrical relaxation data from the tracer diffusion work of Johnson et al. (1951), the electrical modulus data of Provenzano et al. (1972), the conductivity studies of Seddon et al. (1932) and Babcock (1934) and the internal friction data of Day and Steinkamp (1971). T_g calorimetric data from Richet and Bottinga (1984).

of Poole (1948) and Bockris et al. (1955), using the shear modulus data of Mills (1974) via the Maxwell relation (eq. 2); and by the torsional relaxation study of Mills (1974). The fast relaxation is defined by the electrical relaxation data of Provenzano et al. (1972), by the internal friction (torsional) study of Day and Steinkamp (1971), by the Na tracer diffusivity study of Johnson et al. (1951) using:

$$Dt = x^2 \qquad (3)$$

where x is the Na–Na spacing; t is time; and D is the diffusion coefficient) and by the electrical conductivity studies of Seddon et al. (1932) and Babcock (1934), using eq. 3 and the Nernst–Einstein equation:

$$D/\sigma = kT/Ne^2 \qquad (4)$$

where σ is the conductivity; k is Boltzmann's constant; T is temperature; N is Avogadro's number; and e is the atomic charge (e.g., Haven and Verkerk, 1965).

The forms of the structural (mechanical) and the fast relaxations are illustrated by insets a and b (Fig. 1) containing the loss moduli from torsional (Mills, 1974) and electrical (Provenzano et al., 1972) studies, respectively. These loss moduli illustrate the distribution of relaxation times about the mean values that determine the relaxation lines of Fig. 1. The width of these relaxation functions indicates that the detectable distribution of ionic mobilities about the mean is broad (at least $\pm 2 \log_{10}$ units).

The structural relaxation forms a non-Arrhenian curve. This is the time-scale of volume relaxation. At an experimental time-scale of 10^3 s it yields a "glass transition temperature" (e.g., calorimetric data of Richet and Bottinga, 1984) of 724 °C. Experiments performed with dwell times or durations (τ_d) shorter than the structural relaxation time (i.e. to the right of the τ_s curve in Fig. 1) will observe a glass whose volume is unrelaxed ($\tau_d < \tau_s$). The only expansivity mechanisms accessible at temperatures below this curve are the elastic, vibrational components. When the combination of duration and temperature of a diffusion experiment crosses to the left-hand side of the structural relaxation curve then the volume will relax, employing configurational as well as vibrational contributions and any volume- or configuration-dependent property measured across this curve is expected to exhibit an inflection in temperature dependence.

The temperature dependences of alkali diffusion and of electrical conductivity in Na_2O–$3SiO_2$ melt consist of two segments. The lower-temperature electrical conductivity segment is an Arrhenian curve with low activation energy and the upper-temperature segment is non-Arrhenian. The two curves intersect at the point where the duration of the experiment (τ_d) equals the volume relaxation time (τ_s) for the temperature of the experiment. In Fig. 1 the location of this inflection is illustrated using comparison of the electrical conductivity studies of Seddon et al. (1932) and Babcock (1934) and the diffusivity data of Johnson et al. (1951).

The extrapolation of either segment across the inflection will yield incorrect estimates. Similar inflections have been noted previously in both synthetic and natural melts (e.g., Dyment et al., 1987; Braedt and Frischat, 1988). The inflection can be expected to be largest in melts that exhibit strong T_g signals in dilatometry and calorimetry (i.e. large increases in thermal expansivity and heat capacity, respectively) and less strong in glasses such as SiO_2 that exhibit weak T_g signals. Thus, diffusivity data obtained on unrelaxed glasses are not directly comparable with data obtained on relaxed liquids. It is important to emphasize that the temperature of this inflection only corresponds to the calorimetric glass transition temperature because the time-scales of the two types of experiment are similar. Experiments performed on longer time-scales will exhibit a lower-temperature inflection.

5. Observation time-scale (τ_p)

The second consequence of relaxation in silicate liquids concerns the time-scale of cationic diffusion relative to network O and Si diffusion. In a diffusion experiment the jump frequency of the diffusing tracer corresponds to a time-scale that can be considered the characteristic or observational time-scale of the experimental probe (τ_p). In silicate melts all cations are bonded to oxygen. The Eyring diffusivity is controlled by the exchange frequency of Si–O bonds (see Revesz and Schaeffer, 1982; Schaeffer, 1984 for discussion of SiO_2). During such jumps the bonds to cations are temporarily broken and the cation is free to diffuse. At relatively low Eyring mobilities (e.g., high viscosities) the diffusivities of cations are so much faster than network O and Si (Fig. 1) that these atoms appear in fixed structural sites during the average alkali jump. At higher temperatures the cationic and Eyring diffusivities converge until the cationic diffusivities are only 1–2 $\log_{10}$ units higher. At this point Si–O exchanges are occur-
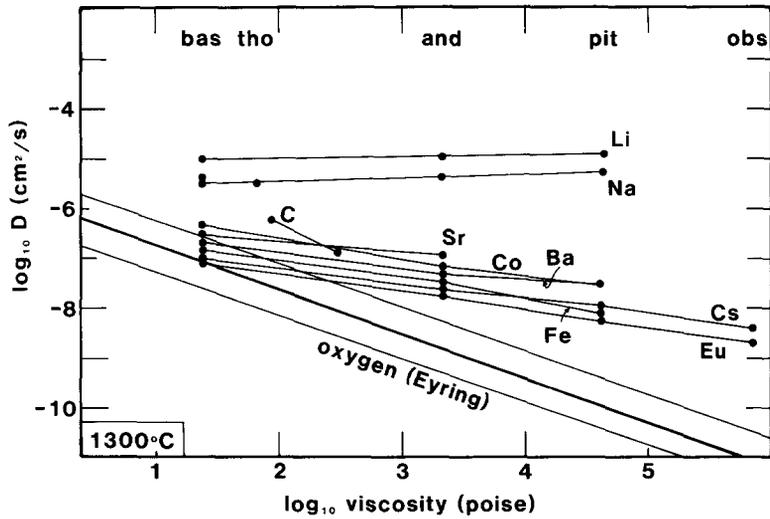
Fig. 2. Cationic tracer diffusivity data (Watson et al., 1982; Henderson et al., 1985) vs. melt viscosity (calculated using the method of Shaw, 1972). The diffusivity of oxygen is calculated from the Eyring relation. All data at 1300°C. Note that the diffusivities of Sr, Co, Ba, Fe, Cs, Eu and C cluster near the calculated Eyring diffusivity.

ring at 1–10% of the frequency of cation jumps and should influence the cationic diffusivities. In the following evidence is presented in support of this effect.

Henderson et al. (1985) have presented tracer diffusivity data for Li, Na, Ba, Co, Sr, Fe, Cs and Eu in basalt, andesite, pantellerite, pitchstone and rhyolite melts. They observed two types of composition dependence of diffusivity. Li and Na exhibit a slight increase in diffusivity with increasing silica content whereas Ba, Co, Fe, Cs, Sr and Eu exhibit a stronger decrease in diffusivity with increasing silica content. The Na and Li data can be explained using the concept of anionic porosity (Dowty, 1980) as increasing silica content from basalt to rhyolite decreases the volume fraction of the melt occupied by oxygen anions. The corresponding increase in free volume or porosity could permit higher diffusivities for cations.

The Sr, Ba, Fe, Cs and Eu data of Henderson et al. (1985) cannot be explained using the anionic porosity concept. The slower cations (Ba, Co, Sr, Fe, Cs, Eu) differ strongly in ionic radii and charge but exhibit similar diffusivity behavior. In Fig. 2 we have plotted the 1300°C diffusivity data of Henderson et al. (1985) as a

function of melt viscosity. The melt viscosities were calculated using the method of Shaw (1972, $\pm 0.5 \log_{10}$ units) and the network O and Si diffusivities, derived from the Eyring equation, are presented as a solid line in Fig. 2. Also included in Fig. 2 are the C tracer diffusion data of Watson et al. (1982) for synthetic Na_2O–Al_2O_3–SiO_2 and basaltic melt. The C data coincide with the slower group of Henderson et al. (1985). The Eyring diffusivity approaches that of Ba, Co, Sr and Cs with decreasing viscosity. The maximum separation, at obsidian, is $< 2 \log_{10}$ units, indicating that the mean jump frequency of oxygen is $> 1\%$ of the cationic jump frequencies. It is important to point out that the diffusivity data represent mean mobilities. The range of mobilities are emphasized in the loss modulus insets a and b of Fig. 1, where the detectable widths of the shear (network O and Si diffusion) and electrical (Na diffusion) relaxation time-scales are $\sim \pm 2 \log_{10}$ units. Thus it is proposed that the compositional dependence of the Co, Sr, Ba, Eu, Fe and C diffusivities at 1300°C (Fig. 2) results from their proximity ($< 2 \log_{10}$ units) to the Eyring diffusivity.

If this proposal is correct then, due to the higher activation energy of network O and Si

diffusion, the Eyring and cationic diffusivities should diverge at higher viscosities. In this event the diffusivities of the slower cations should bear no relationship to viscosity. Instead, they might be positive functions of silica content or anionic porosity (as is the case for Na and Li). Fig. 3 demonstrates that this occurs, using diffusivity data over an extended (higher) range of melt viscosities, from basalt to SiO_2, at 1000°C. The Ca, Sr and Ba diffusivity data (Jambon and Carron, 1976, 1978; Hofmann and Magaritz, 1977; Magaritz and Hofmann, 1978; Jambon, 1982) in Fig. 3 exhibit a composition dependence similar to that of Na, in direct contrast to the composition dependence of Ba and Sr diffusion at 1300°C (Fig. 2). It is proposed, therefore, that at 1000°C, the Ca, Sr and Ba diffusivities are too far removed from oxygen mobility to be affected by it and the compositional dependence of Ca, Ba and Sr in an static oxide matrix is being observed.

Also illustrated in Fig. 3 are diffusivity data for Al, Fe, Ni and Si in SiO_2 glass and for Si in a $CaO-Al_2O_3-SiO_2$ melt (Frischat, 1969, 1975; Ghoshtagore, 1969; Brebec et al., 1980; Atkinson and Gardner, 1980). The diffusivities of Al, Fe and Ni in SiO_2 are removed from the Eyring

diffusivity and thus they are predicted to have decreasing diffusivity with decreasing silica content, until their diffusivity approaches the Eyring curve. The diffusivity of Si lies on the Eyring diffusivity curve both for SiO_2 and for the Ca-Al-Si melt (at viscosities 14 orders of magnitude in difference). These data indicate that Si diffusivity is being influenced by the exchange frequency of oxygen anions over the entire range of this comparison. (The case for O is complicated by the presence of physically dissolved oxygen in the melts at high O_2 pressures, e.g., Schaeffer, 1984.)

The inset of Fig. 3 illustrates the three possible cases of composition dependence expected from the previous discussion. In case a, the slight positive dependence of diffusivity of silica content is unrelated to viscosity (e.g., Na and Li in Figs. 2 and 3). In case c the cationic diffusivity follows the Eyring line (e.g., Si in Fig. 3). The intermediate case b, detached cationic diffusivity at high viscosity and Eyring diffusivity at low viscosity, is the behavior observed for Ba and Sr and expected for Al, Fe, Ni, Eu, Co and possibly C.

Finally, self-diffusivity can also be approximated in binary interdiffusion experiments
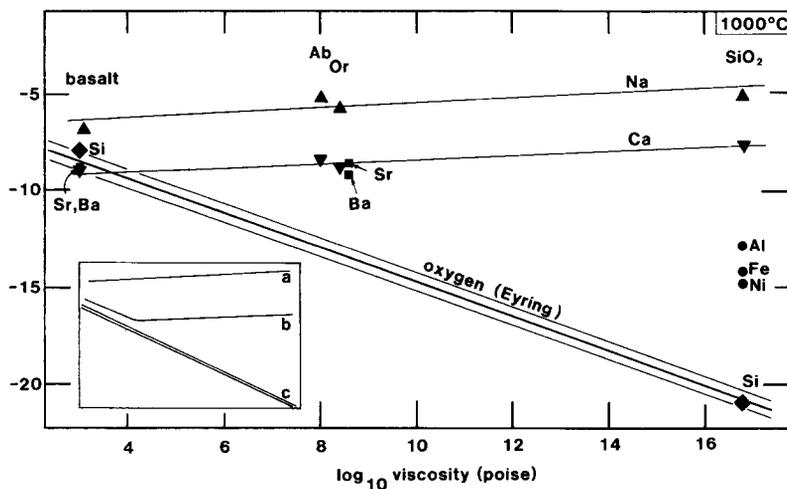
Fig. 3. Tracer diffusivity data vs melt viscosity for basalt, a Ca-Al-Si synthetic oxide melt, albite and orthoclase melts, and SiO_2 melt at 1000°C. Note that the composition dependence of Ca diffusivity is a slight positive dependence on SiO_2 content, apparently unrelated to viscosity.

where the compositional difference between the diffusion end-members is small. Baker and Watson (1988) have reported that the diffusivity of Al, Fe, Si, Mn, Zn, Y, Zr and Nb are all within an order of magnitude at 900–1400°C in the rhyolitic melts of their study. Calculated Eyring diffusivities for their melts are within a log unit of these cationic values. Thus it is proposed that the tight clustering of cationic diffusivities observed in that study result from the value of Eyring diffusivity.

6. Conclusions

Diffusion experiments, like all other property determinations on silicate melts, have two characteristic time-scales which must be considered with respect to structural relaxation; namely, the experimental duration (τ_d) and the observation time-scale (τ_p, in this case the inverse of the diffusive jump frequency). As a result, two effects involving the glass transition influence the temperature- and composition dependence of cationic tracer diffusivities in silicate melts. The first effect is an inflection in the temperature dependence of diffusivity that occurs when the time duration of the experiment intersects the volume relaxation time ($\tau_d = \tau_s$). The result is enhanced diffusivities at higher temperature. The second effect is an inverse viscosity dependence of the cationic tracer diffusivities which occurs when the jump frequency of oxygen diffusion approaches the jump frequency of cationic tracer diffusion ($\tau_p = \tau_s$). The cations can be viewed as diffusing in a static glass matrix below this temperature and in a dynamic liquid matrix above this temperature. The diffusivity behavior of cations of various geochemical affinities converge due to the dominating effect of network O and Si diffusivity.

Acknowledgements

References

Angell, C.A., 1988. Structural instability and relaxation in liquid and glassy phases near the fragile liquid limit. J. Non-Cryst. Solids, 102: 205–221.

Atkinson, A. and Gardner, J.W., 1980. At. Energy Res. Establish., Harwell, AERE R-9684.

Babcock, C.L., 1934. Viscosity and electrical conductivity of molten glasses. J. Am. Ceram. Soc., 17: 329–342.

Baker, D.R. and Watson, E.B., 1988. Diffusion of major and trace elements in compositionally complex Cl- and F-bearing silicate melts. J. Non-Cryst. Solids, 102: 62–70.

Bockris, J. O'M., MacKenzie, J.D. and Kitchener, J.A., 1955. Viscous flow in silica and binary liquid silicates. Trans. Faraday Soc., 51: 1734–1748.

Braedt, M. and Frischat, G.H., 1988. Sodium self diffusion in glasses and melts of the system Na_2O–Rb_2O–SiO_2. Phys. Chem. Glass, 29: 214–218.

Brebec, G., Seguin, R., Sella, C., Bevenot, J. and Martin, J.C., 1980. Diffusion du silicium dans la silice amorphe. Acta Metall., 28: 327–333.

Day, D.E. and Steinkamp, W.E., 1971. In: E.A. Porai-Koshits (Editor), Stekloobraznoye Sostoyaniye. Leningrad, pp. 294–298.

Dingwell, D.B. and Webb, S.L., 1989. Structural relaxation in silicate melts and non-Newtonian melt rheology in geologic processes. Phys. Chem. Mineral., 16: 508–516.

Dingwell, D.B. and Webb, S.L., 1990. Relaxation in silicate melts. Eur. J. Mineral. (in press).

Dowty, E., 1980. Crystal-chemical factors affecting the mobility of ions in minerals. Am. Mineral., 65: 174–182.

Dyment, F., Matzke, Hj. and Toscano, E., 1987. Diffusion of ^{83}Rb and ^{84}Rb tracers in waste glasses. J. Non-Cryst. Solids, 93: 22–34.

Frischat, G.H., 1969. Evidence for calcium and aluminum diffusion in SiO_2 glass. J. Am. Ceram. Soc., 52: 625.

Frischat, G.H., 1975. Ionic Diffusion in Oxide Glasses. Diffusion Monograph Series, 3/4. Trans Tech Publications, Aedermannsdorf, 182 pp.

Ghoshtagore, R.N., 1969. Diffusion of nickel in amorphous silicon dioxide and silicon nitride films. J. Appl. Phys., 40: 4374–4376.

Glasstone, S., Laidler, K.J. and Eyring, H., 1941. The Theory of Rate Processes. McGraw-Hill, New York, N.Y., 611 pp.

Haven, Y., Verkerk, B., 1965. Diffusion and electrical conductivity of sodium ions in sodium silicate glasses. Phys. Chem. Glass, 6: 38–45.

Henderson, P., Nolan, J., Cunningham, G.C. and Lowry, R.K., 1985. Structural controls and mechanisms of diffusion in natural silicate melts. Contrib. Mineral. Petrol., 89: 263–272.

Höfler, S. and Seifert, F.A., 1984. Volume relaxation of compacted glass: a model for the conservation of natural diaplectic glasses. Earth Planet. Sci. Lett., 67: 433–438.

Hofmann, A.W. and Magaritz, M., 1977. Diffusion of Ca, Sr, Ba and Co in a basaltic melt: implications for the geochemistry of the mantle. J. Geophys. Res., 82: 5432–5440.

Jambon, A., 1982. Tracer diffusion in granitic melts: experimental results for Na, K, Rb, Cs, Ca, Sr, Ba, Ce, Eu to 1300°C and a model for calculation. J. Geophys. Res., 87: 10797–10810.

Jambon, A. and Carron, J.P., 1976. Diffusion of Na, K, Rb and Cs in glasses of albite and orthoclase composition. Geochim. Cosmochim. Acta, 40: 897–903.

Jambon, A. and Carron, J.P., 1978. Étude expérimentale de la diffusion cationique dans un verre basaltique: alcalins et alcalino-terreux. Bull. Minéral., 101: 22–96.

Johnson, J.R., Bristow, R.H. and Blau, H.H., 1951. Diffusion of ions in some simple glasses. J. Am. Ceram. Soc., 34: 165–172.

Li, J.H. and Uhlmann, D.R., 1970. The flow of glass at high stress levels. J. Non-Cryst. Solids, 33: 235–248.

Liu, S-B., Stebbins, J.F., Schneider, E. and Pines, A., 1988. Diffusive motion in alkali silicate melts: an NMR study at high temperature. Geochim. Cosmochim. Acta, 52: 527–538.

Magaritz, M. and Hofmann, A.W., 1978. Diffusion of Sr, Ba and Na in obsidian. Geochim. Cosmochim. Acta, 42: 595–605.

Mills, J.J., 1974. Low frequency storage and loss moduli of soda silica glasses in the transformation range. J. Non-Cryst. Solids, 14: 255–268.

Poole, J.P., 1948. Viscosité à basse température des verre alcalino-silicates. Verres Réfract., 2: 222–228.

Provenzano, V., Boesch, L.P., Volterra, V., Moynihan, C.T. and Macedo, P.B., 1972. Electrical relaxation in Na_2O–$3SiO_2$ glass. J. Am. Ceram. Soc., 55: 492–496.

Revesz, A.G. and Schaeffer, H.A., 1982. The mechanism of oxygen diffusion in vitreous SiO_2. J. Electrochem. Soc., 129: 357–361.

Richet, P. and Bottinga, Y., 1984. Anorthite, andesine, wollastonite, diopside, cordierite and pyrope: thermodynamics of melting, glass transitions, and properties of the amorphous phases. Earth Planet. Sci. Lett., 67: 415–432.

Ritland, H.N., 1954. Density phenomena in the transformation range of a borosilicate crown glass. J. Am. Ceram. Soc., 37: 370–378.

Schaeffer, H.A., 1984. Diffusion-controlled processes in glass-forming melts. J. Non-Cryst. Solids, 67: 19–33.

Scherer, G.W., 1984. Relaxation in Glass and Composites. Wiley, New York, N.Y., 331 pp.

Seddon, E., Tippet, E.J. and Turner, W.E.S., 1932. Electrical conductivity of sodium-metasilicate glasses. J. Soc. Glass Technol., 16: 450–477.

Shaw, H.R., 1972. Viscosities of magmatic silicate liquids: an empirical method of prediction. Am. J. Sci., 272: 870–893.

Shimizu, N. and Kushiro, I., 1984. Diffusivity of oxygen in jadeite and diopside melts at high pressures. Geochim. Cosmochim. Acta, 48: 1295–1303.

Simmons, J.H., Mohr, R.K. and Montrose, C.J., 1982. Non-Newtonian viscous flow in glass. J. Appl. Phys., 53: 4075–4080.

Stebbins, J.F., 1988. Effects of temperature and composition on silicate glass structure and dynamics: Si-29 NMR results. J. Non-Cryst. Solids, 106: 359–369.

Watson, E.B., Sneeringer, M.A. and Ross, A., 1982. Diffusion of dissolved carbonate in magmas: experimental results and applications. Earth Planet. Sci. Lett., 61: 346–358.

Webb, S.L. and Dingwell, D.B., 1990a. Non-Newtonian viscosities of geologic melts at high stresses: experimental results for rhyolite, andesite, basalt and nephelinite. J. Geophys. Res. (in press).

Webb, S.L. and Dingwell, D.B., 1990b. The onset of non-Newtonian rheology in silicate melts: a fiber elongation study. Phys. Chem. Miner. (in press).